J|A|C|S
ARTICLES
Published on Web 07/29/2003

Nanowells on Silica Particles in Water Containing Long-Distance Porphyrin Heterodimers

Guangtao Li,[†] Sheshanath V. Bhosale,[†] Tianyu Wang,[†] Steffen Hackbarth,[‡] Beate Roeder,[‡] Ulrich Siggel,[§] and Jürgen-Hinrich Fuhrhop*,[†]

Contribution from the Freie Universität Berlin FB Biologie, Chemie, Pharmazie Institut für Chemie/Organische Chemie, Takustr. 3 D-14195 Berlin, Germany, Humboldt-Universität zu Berlin Mathematisch-Naturwissenschaftliche Fakultät I Institut für Physik (Photobiophysik), Invalidenstr. 110 10115 Berlin, Germany and Max-Volmer Institut für Physikalische Chemie der Technischen Universität Berlin, Strasse des 17. Juni 135, D-10623 Berlin, Germany

Received April 10, 2003; E-mail: Fuhrhop@chemie.fu-berlin.de

Abstract: Smooth and nonswelling spherical silica particles with a diameter of 100 nm and an aminopropyl coating are soluble in water at pH 11, coagulate quickly at pH 3, and redissolve at pH 9. Electron microscopy as well as visible spectra of covalently attached porphyrins indicate the aggregation state of the particles. Long-chain α,ω-dicarboxylic acids with a terminal oligoethyleneglycol (═OEG)-amide group were attached in a second self-assembly step to the remaining amine groups around the porphyrins. Form-stable 2-nm wells were thus obtained and were characterized by fluorescence quenching experiments using the bottom porphyrin as a target. The one-dimensional diffusion of fitting quencher molecules along the 2-nm pathway took several minutes. Porphyrins with a diameter above 2 nm could not enter the form-stable gaps at all. Added tyrosine stuck irreversibly to the walls of the nanowells and prevented the entrance of quencher molecules, the OEG-headgroups fixated 2,6-diaminoanthraquinone. A ring of methylammonium groups was then fixed at the walls of the wells at a distance of 5 or 10 Å with respect to the bottom porphyrin. 2,6-Disulfonatoanthraquinone was attached only loosely to this ring, but the exactly fitting manganese(III) *meso*-(tetraphenyl-4-sulfonato)porphyrinate (Mn(III) TPPS) was tightly bound. Transient fluorescence experiments showed a fast decay time of 0.2 ns for the bottom porphyrin, when the Mn(III) TPPS was fixated at a distance of 5 Å. Two different dyes have thus been immobilized at a defined subnanometer distance in an aqueous medium.

1. Introduction

Long-distance (∼6−20 Å) molecular pairs consisting of a photoactive electron donor and an electron acceptor are promising systems for light-induced charge separation. They may eventually lead to large-scale preparations which allow the splitting of water into hydrogen and oxygen or related oxidants. Noncovalent assemblies in fluid[1] or rigid[2−5] 2-nm gaps in surface monolayers on gold have been developed as carriers for such heterodimers of metalloporphyrins on gold platelets and colloidal nanoparticles.[2−5] The plasmon absorption and heating of colloidal gold produced[5] caused serious artifacts in flash photolysis experiments, which are also to be expected for semiconducting nanoparticles.[6]

We therefore turned to photoinactive coated silica particles. They are colorless, do not quench the porphyrin's fluorescence, and can be made under a variety of conditions with different coatings. The smoothness, size, and chemical self-assembly procedures were optimized in order to establish a closed monolayer with modest curvature and containing functional gaps.[3,7] First experiments proved that the mixed rigid monolayer on silicagel can be successfully applied (i) for flash photolysis experiments in water, (ii) for enhancing the lifetime of porphyrin triplet states by a factor of 10, (iii) for the study of 2D diffusion of fluorescence quenching molecules on a variety of surfaces and 1D diffusion in pores using standard spectrometers, (iv) for the analysis of reversible particle aggregation by UV/vis and fluorescence spectroscopy, (v) for the establishment of nanometer-sized containers, which can be closed and opened

[†] Freie Universität Berlin FB Biologie, Chemie, Pharmazie Institut für Chemie/Organische Chemie.

[‡] Humboldt-Universität zu Berlin Mathematisch-Naturwissenschaftliche Fakultät I Institut für Physik (Photobiophysik).

[§] Max-Volmer Institut für Physikalische Chemie der Technischen Universität Berlin.

(1) (a) Sagiv, J. *Isr. J. Chem.* **1979**, *18*, 346. (b) Sagiv, J. *J. Am. Chem. Soc.* **1980**, *102*, 92.
(2) Kang, J. F.; Ulman, A.; Liao, S.; Jordan, R. *Langmuir* **1999**, *15*, 2095.
(3) Li, G.; Fudickar, W.; Skupin, M.; Klyszcz, A.; Draeger, C.; Lauer, M.; Fuhrhop, J.-H. *Angew. Chem.* **2002**, *114*, 1906; *Angew. Chem., Int. Ed.* **2002**, *41*, 1828.
(4) (a) Skupin, M.; Li, G.; Fudickar, W.; Zimmermann, J.; Roeder, B.; Fuhrhop, J.-H. *J. Am. Chem. Soc.* **2001**, *123*, 3454. (b) Fudickar, W.; Zimmermann, J.; Ruhlmann, L.; Roeder, B.; Siggel, U.; Fuhrhop, J.-H. *J. Am. Chem. Soc.* **1999**, *121*, 9539.
(5) (a) Li. G.; Fuhrhop, J.-H. *Langmuir* **2002**, *18*, 7740. (b) Li, G.; Lauer, M.; Schulz, A.; Boettcher, C.; Li, F.; Fuhrhop, J.-H., submitted for publication.
(6) Fendler, J. H., Ed. *Nanoparticles and Nanostructured Films*; Wiley-VCH: 1998.
(7) (a)Fuhrhop, J.-H.; Koening, J., *Molecular Assemblies and Membranes*; Stoddard, J. F., Ed.; *Monographs in Supramolecular Chemistry*; Royal Soc. Chem.: London, 1994. (b) Fuhrhop, J.-H.; Endisch, C. *Molecular and Supramolecular Chemistry of Natural Products and Model Compounds*; Marcel Dekker: New York, 2000.

by pH changes, and, (vi) most interestingly, for the establishment of long-distance redox pairs in aqueous medium. Their advantage with respect to assembled polymer capsules,[8] which serve similar purposes, is the rigidity of the membrane gaps, which allows adjustment of the distance between components within a few angströms.

2. Experimental Section

Synthesis. Toluene-4-sulfonic Acid 2-{2-[2-(2-Methoxyethoxy]-ethoxy}ethyl Ester. Tri(ethylene glycol)monomethyl ether (2 g, 10 mmol) was suspended in dry pyridine (10 mL) at 0 °C under an argon atmosphere. 4-Methylbenzenesulfonyl chloride (3.9 g, 20 mmol) was added at room temperature. The resulting mixture was stirred for 24 h at room temperature. The reaction mixture was poured into 20 mL of water, the resulting suspension was extracted with CH_2Cl_2, and the extract was dried with magnesium sulfate; evaporation followed by flash chromatography (ethyl acetate) afforded white solids, 3.0 g (88%). ^{1}H NMR (270 MHz, $CDCl_3$) δ 2.4 (s, 3H), 3.24 (s,3H, CH_3O), 3.79−3.59 (m, 14 H), 3.56 (t, 2H, CH_2O), 3.70 (t, 2H, CH_2O), 7.34(d, 2H, aromatic), 7.73 (d, 2H, aromatic).

1-{2-[2-(2-Azidoethoxy)ethoxy]ethoxy}-2-methoxyethane. Sodium azide (1.1 g, 16.5 mmol) was added to a solution of toluene-4-sulfonic acid 2-{2-[2-(2-methoxyethoxy]ethoxy}ethyl ester (3.0 g, 11 mmol) in dry DMF (12 mL). The mixture was heated at 90 °C for 6 h and then allowed to attain room temperature. The DMF was evaporated, and the residue was purified by flash chromatography (ethyl acetate) giving 2.26 g (94%) of compound as a light yellow oil. ^{1}H NMR (270 MHz, $CDCl_3$) δ 3.2 (t, 2H, CH_2N_3), 3.4 (t, 2H, CH_2O), 3.24 (s, 3H, CH_3O), 3.56−3.62 (m, 12H, OCH_2CH_2O).

1-{2-[2-(2-Azidoethoxy)ethoxy]ethoxy}ethylamine (1). A solution of 1-{2-[2-(2-azidoethoxy)ethoxy]ethoxy}-2-methoxyethane (1.3 g, 5.58 mmol) in dry THF (30 mL) was cooled to 0 °C. Triphenyl phosphine was added (1.8 g, 7.0 mmol), after which the mixture was allowed to stand at room temperature for 24 h. Water (0.4 mL) was added, and the reaction mixture was stirred for another 24 h to hydrolyze the intermediate phosphorus adduct. The reaction mixture was diluted with water and washed with toluene. Evaporation of the aqueous layer yielded 1.1 g (97%) of compound as a pale yellow oil. ^{1}H NMR (270 MHz, $CDCl_3$) δ 1.5 (broad, 2H, NH_2), 2.87 (broad, 2H, CH_2NH_2), 3.24 (s, 3H, CH_3O), 3.6 (t, 2H, CH_2O), 3.56−3.63 (m, 12H, OCH_2CH_2O); ^{13}C NMR (63 MHz, $CDCl_3$) δ 41.1, 58.3, 69.0, 69.5, 69.6, 69.8, 69.9, 70.29, 71.3.

12-Oxododecanoic Acid Benzyl Ester (2b). A solution of 12-hydroxydodecanoate acid (10 g, 26.3 mmol) in 120 mL of DMF was treated with potassium bicarbonate (5.10 g, 50.92 mmol) and benzyl bromide (9.12 g, 53.24 mmol) and stirred at rt for 24 h. The solvent was removed under reduced pressure. The resulting mixture was partitioned between ethyl acetate and aqueous HCl. The organic phase was separated, washed with water, and dried with $MgSO_4$. Removal of the solvent in a vacuum resulted in a solid, which was recrystallized in methanol to afford white crystals in a yield of 8.50 g. ^{1}H NMR (270 MHz, $CDCl_3$) δ 1.36 (m, 14H, 7 × CH_2), 1.57 (m, 4H, 2 × CH_2), 2.38 (t, 2H, CH_2COO), 3.63 (t, 2H, CH_2OH), 5.11 (s, 2H, CH_2Ph), 7.38 (s, 5H, aromatic); ^{13}C NMR (63 MHz, $CDCl_3$) δ 24.8, 25.6, 28.9, 29.0, 29.3, 29.4, 29.5, 32.6, 34.2, 62.7, 65.9, 128.0, 128.4, 136.0, 173.6; MS *m*/*z* 306 (M), 278 (M − CO). Pyridinium chlorochromate (3.23 g, 15 mmol) was suspended in 100 mL of CH_2Cl_2, and the above benzyl ester (3.50 g, 10 mmol) was rapidly added at room temperature. After 1.5 h, the oxidation was completed (monitored by TLC). The black reaction mixture was diluted with 300 mL of anhydrous ether, the solvent was decanted, and the black solid was washed twice with ether. The product was isolated simply by filtration of the organic extracts through Florisil, and evaporation of the solvent at reduced pressure affords the product in a yield of 3.15 g as an oil. ^{1}H NMR (270 MHz, $CDCl_3$) δ 1.35 (m, 12H, 6 × CH_2), 1.57 (m, 4H, 2 × CH_2), 2.40 (m, 4H, CH_2COO, CH_2OH), 5.10 (s, 2H, CH_2Ph), 7.40 (s, 5H, aromatic), 9.77 (s, 1H, COH); ^{13}C NMR (63 MHz, $CDCl_3$) δ 21.9, 24.8, 29.0, 29.1, 29.2, 34.2, 43.7, 65.9, 128.0, 128.4, 136.0, 173.5, 202.8; MS *m*/*z* 304 (M), 276 (M − CO).

Tetradec-2-enedioic Acid 14-Benzyl Ester (3b). Sodium hydride (1.32 g, 32.90 mmol) was suspended in 100 mL of THF at 0 °C under an argon atmosphere. *tert*-Butyl-*P*,*P*-dimethylphosphono acetate (7.38 g, 32.90 mmol) was added dropwise at this temperature. After the evolution of H_2 bubbles had ceased, a solution of (10 g, 32.90 mmol) 14-oxy-tetradec-12-enoic acid benzyl ester (**2b**) in 50 mL of THF was added slowly. The resulting mixture was stirred for 24 h. The solvent was removed under reduced pressure, and the residue was taken up with water. After extraction with four portions of ether and subsequent drying, a white solid was obtained which was recrystallized from hexane to give 9.80 g of product. ^{1}H NMR (270 MHz, $CDCl_3$) δ 1.30 (m, 12H, 6 × CH_2), 1.44 (s, 9H, $(CH_3)_3C$), 1.58 (m, 4H, 2 × CH_2), 2.30 (m, 4H, 2 × CH_2), 5.10 (s, 2H, CH_2Ph), 5.73 (d, 1H, vinyl α-H), 6.87 (dt, 1H, vinyl β-H), 7.41 (s, 5H, aromat.); ^{13}C NMR (63 MHz, $CDCl_3$) δ 24.8, 28.0, 28.1, 28.5, 28.7, 28.9, 29.0, 29.1, 29.3, 31.9, 34.2, 65.9, 79.8, 122.8, 128.0, 128.4, 136.0, 148.0, 166.7, 173.5; MS (FAB neg., Xe) *m*/*z* 682 (M), 653 (M − CO). Toluene solution (100 mL) containing 5 g of the above butyl ester (14.45 mmol) and 5 g of *p*-toluenesulfonic acid was refluxed for 30 min and subsequently stirred at room temperature overnight. After toluene was removed, 300 mL of 5% aqueous potassium bicarbonate solution was added and stirred for 10 min. The white precipitate was filtered off, and the filtrate was acidified to pH 3 with dilute HCl. The resulting suspension was extracted with chloroform and dried with magnesium sulfate. After the removal of solvent in vacuo, the resulting solid was recrystallized from chloroform/hexane to give 3.95 g of white crystals. ^{1}H NMR (270 MHz, $CDCl_3$) δ 1.33 (m, 12H, 6 × CH_2), 1.48 (m, 2H, CH_2), 1.61 (m, 2H, CH_2), 2.20 (m, 2H, CH_2), 2.38 (t, 2H, CH_2COO), 5.10 (s, 2H, CH_2Ph), 5.73 (d, 1H, vinyl α-H), 6.87 (dt, 1H, vinyl β-H), 7.41 (s, 5H, aromat.), 11.60 (m, 1H, COOH);^{13} C NMR (63 MHz, $CDCl_3$) δ 24.8, 27.7, 28.5, 29.1, 29.2, 29.3, 29.4, 32.2, 34.2, 66.0, 120.4, 128.0, 128.4, 136.0, 152.2, 172.0, 173.6; MS (FAB, pos, Xe) *m*/*z* 347 (M), 329 (M − H_2O).

13-(2-{2-[2-(2-Methoxyethoxy)ethoxy]ethoxy}ethylcarbamoyl)-tridec-12-enoic Acid Benzyl Ester (4b). Compounds **1** (0.595 g, 2.89 mmol) and **3b** (1 g, 2.89 mmol) were dissolved in 200 mL of CH_2Cl_2. After the solution was cooled to 0 °C for 15 min, DCC (1.48 g, 7.22 mmol) and DMAP (1 g, 9 mmol) were added. The reaction mixture was then stirred at room temperature for 24 h further. The white precipitate was filtered off, and the filtrate was washed successively with 0.1 M HCl, 8% $NaHCO_3$, and water and dried over $MgSO_4$. The solvent was removed in a vacuum, and the residue was purified by silica column chromatography using CH_2Cl_2/MeOH (10:1) as eluent, followed by crystallization from hexane/ethyl acetate. Yield: 1.3 g as a white solid (84.9%). ^{1}H NMR (270 MHz $CDCl_3$) δ 1.24 (m, 12H, 6 × CH_2), 1.49 (m, 4H, CH_2), 1.63 (m, 2H, allyl-H), 2.37 (t, 2H, CH_2-COO), 3.45 (s, 3H, CH_3−O), 3.56 (m, 2H, CH_2NH), 3.56−3.7 (m, 14H, CH_2O), 5.08 (s, 2H, CH_2Ph), 5.73 (d, 1H, vinyl α-H), 6.30 (broad, 1H, NH), 6.87 (dt, 1H, vinyl β-H), 7.41 (s, 5H, aromat.); MS (FAB neg., Xe) *m*/*z* 536 (M + H).$^+$

13-(2-{2-[2-(2-Methoxyethoxy)ethoxy]ethoxy}ethylcarbamoyl)-tridec-12-enoyl Chloride (5b). Benzyl ester **4b** (1.2 g) was treated with 25 mL of LiOH (1 M) suspension in 10 mL of THF, 5 mL of

(8) Dai, Z.; Dahne, L.; Donath, E.; Möhwald, H. *Langmuir* **2002**, *18*, 4553.
(9) (a) Cao, G.; Rabenberg, L. K.; Nunn, C. N.; Mallouk, T. E. *Chem. Mater.* **1991**, *3*, 149. (b)Yang, H. C.; Aoki, K.; Hong, H.-G.; Sackett, D. D.; Arendt, M. F.; Yau, S.-L.; Bell, C. M.; Mallouk, T. E. *J. Am. Chem. Soc.* **1993**, *115*, 11855.
(10) van Blaaderen, A.; Vrij, A. J. *Coll. Interfacial Sci.* **1993**, *156*, 1.
(11) For convex surfaces: Klyszcz, A. Ph.D. Thesis, FU: Berlin, 2001, p 99ff.
(12) for concave surfaces: Shin, Y.; Liu, J.; Wang, L.-Q.; Nie, Z.; Samuels, W. D.; Fryxell, G. E.; Exarhos, G. J. *Angew. Chem.* **2000**, *112*, 2814.
(13) Pekharinen, L.; Linschitz, H. *J. Am. Chem. Soc.* **1960**, *82*, 2407.

methanol, and 5 mL of water. The resulting mixture was stirred overnight at room temperature. After removal of the solvent in vacuo, the mixture was extracted with ethyl acetate and water. The aqueous phases were combined and acidified to pH 2 with dilute HCl. The suspension was extracted with chloroform, dried with $MgSO_4$, and evaporated to afford 1 g of white crystal. ^{1}H NMR (270 MHz $CDCl_3$) δ 1.24 (m, 12H, 6 × CH_2), 1.49 (m, 4H, CH_2), 1.63 (m, 2H, allyl-H), 2.37 (t, 2H, CH_2COO), 3.45 (s, 3H, CH_3−O), 3.56 (m, 2H, CH_2NH), 3.56−3.7(m, 14H, OCH_2CH_2O), 5.89 (d, 1H, vinyl α-H), 6.5 (m, 1H, NH), 6.87 (dt, 1H, vinyl β-H); ^{13}C NMR (63 MHz, $CDCl_3$) δ 24.8, 27.7, 28.5, 29.1, 29.2, 29.3, 29.4, 32.2, 34.2, 66.0, 62.45, 64.56, 69.67, 69.84, 70.11, 70.20, 71.60, 76.49, 77.00, 77.50, 120.4, 128.0, 128.4, 136.0, 152.2, 177.0; MS (FAB neg., Xe) *m*/*z* 446 $(M + H)^+$.

Compound **5b** (0.1 g) was dissolved in CH_2Cl_2 and mixed at 0 °C with 2 equiv of oxalyl chloride. After the mixture was stirred at this temperature for 1 h, it was slowly brought to room temperature and stirred overnight. Removal of the solvent under low pressure afforded the product.

6-Oxohexanoic Acid Ethyl Ester (2a). This compound was synthesized from the benzyl ester given above by the same method described for **2b**. Yield: 83% of an oil. ^{1}H NMR (270 MHz, $CDCl_3$) δ 1.12 (3H, t), 1.35 (m, 2H, 1 × CH_2), 1.57 (m, 2H, 1 × CH_2), 2.40 (m, 4H, CH_2COO u. CH_2OH), 4.1 (2H, q), 9.77 (s, 1H, CHO).

8-Ethyloxynona-2,8-dienoic Acid (3a). This compound was synthesized from **2a** by the same method described for **3b** as a white solid yield (89%). *tert*-Butyl ester: ^{1}H NMR (270 MHz, $CDCl_3$) δ 1.12 (3H, t), 1.35 (m, 2H, 1 × CH_2), 1.44 (s, 9H, $(CH_3)_3C$), 1.58 (m, 2H, 2 × CH_2), 2.30 (m, 4H, 2 × CH_2), 4.1 (2H, q), 5.73 (d, 1H, vinyl α-H), 6.87 (dt, 1H, vinyl β-H). This free acid was recrystallized from CH_2Cl_2/hexane to afford a white solid with a yield of 84%. ^{1}H NMR (270 MHz, $CDCl_3$) δ 1.12 (3H, t), 1.33 (m, 2H, 1 × CH_2), 1.48 (m, 2H, CH_2), 2.20 (m, 2H, CH_2), 2.38 (t, 2H, CH_2COO), 4.1 (2H, q), 5.73 (d, 1H, vinyl α-H), 6.87 (dt, 1H, vinyl β-H), 8.0 (m, 1H, COOH).

7-(2-{2-[2-(2-Methoxyethoxy)ethoxy]ethoxy}ethylcarbamoyl)-hept-6-enoic Acid Ethyl Ester (4a). This compound was synthesized from **1** and **3a** by the same method as described for **4b** as a white solid with yield (78%). ^{1}H NMR (270 MHz $CDCl_3$) δ 1.12 (3H, t), 1.34 (m, 2H, 1 × CH_2), 1.49 (m, 2H, CH_2), 1.63 (m, 2H, allyl-H), 2.37 (t, 2H, CH_2COO), 3.45 (s, 3H, CH_3O), 3.56 (m, 2H, CH_2NH), 3.56−3.7 (m, 14H, CH_2O), 4.1 (2H, q), 5.73 (d, 1H, vinyl α-H), 6.30 (m, 1H, NH), 6.87 (dt, 1H, vinyl β-H).

7-(2-{2-[2-(2-Methoxyethoxy)ethoxy]ethoxy}ethylcarbamoyl)-hept-6-enoyl Chloride (5a). This compound was synthesized from **4a** using the same method as described for **5b**. ^{1}H NMR of acid (270 MHz $CDCl_3$) δ 1.34 (m, 2H, 1 × CH_2), 1.49 (m, 2H, CH_2), 1.63 (m, 2H, allyl-H), 2.37 (t, 2H, CH_2COO), 3.45 (s, 3H, CH_3O), 3.56 (m, 2H, CH_2NH), 3.56−3.7(m, 14H, OCH_2CH_2O), 5.89 (d, 1H, vinyl α-H), 6.5 (m, 1H, NH), 6.87 (dt, 1H, vinyl β-H); MS(FAB) *m*/*z* 362 $(M + H)^+$.

Preparation of Amino Modified Silica Colloids. Colloidal silica nanoparticles with a mean diameter of 100 nm were prepared according to standard method with slight modification. All glass reaction vessels were cleaned extensively to ensure that no nucleation sites were present (washing procedure: filling with 3% hydrofluoric acid for an hour, rinsing with Milli-Q water and finally rinsing with distilled ethanol). In a reaction vessel, which had been dried for 3 h at 120 °C, TEOS (1.5 mL) and ammonia (3 mL, 28%) were dissolved in 50 mL of anhydrous ethanol, and the reaction mixture was slowly stirred at room temperature for 24 h in the dark. Milli-Q water (400 μl) was added and stirred for 2 h further. Then, (3-Aminopropyl)triethoxy silicate (APTS) (400 μl) was given, and the mixture was stirred overnight. The resulting silica sol was warmed to 80 °C and refluxed at this temperature for 10 h under an argon atmosphere. The amino-modified silica colloids with a diameter of 100 nm were used for self-assembling work after cooling to room temperature.

Preparation of Closed Membranes and Construction of Nanogaps on Silica Colloidal Particles. Silica particles coated with gaps and closed membranes were prepared as follows: The above-mentioned silica colloid (0.5 g) was washed 4 times with anhydrous ethanol and anhydrous CH_2Cl_2 by repeated centrifugation, dispersion, and ultrasonification. Then, obtained silica particles were dissolved in 50 mL of CH_2Cl_2 containing 1 mL of dry triethylamine. With vigorous stirring, 4 mL of CH_2Cl_2 solution of porphyrin **11** (1 mg) was added dropwise. After the mixture was stirred for 2 h, 5 mL of CH_2Cl_2 solution of bola **5a** or **5b** (2 mg) were given. The resulting suspension was stirred in the dark overnight. The membrane coated nanoparticles were isolated by repeated centrifugation, dispersion, and ultrasonification using CH_2Cl_2 as solvent and were used for further measurements.

Functionalization of Nanogaps on Silica Particles. Amino groups were introduced on the wall of nanogaps by Michael addition of methylamine to the activated double bond of bola **5a** and **5b** on silica particles. Briefly, gaps-coated silicate particles prepared above were dispersed in 10 mL of an aqueous solution of methylamine (10 mM). After the mixture was stirred for 2 h, the silica particles were collected by centrifugation and washed several times using Milli-Q water.

Construction of Porphyrin Heterodimer on Silica Particle. Porphyrin heterodimers separated by a defined distance were established on silica particles as follows. Silica particles (0.5 g) with amino functionalized gaps were dispersed in 5 mL of Milli-Q water, and porphyrin **9** (Mn(III) TPPS) (0.1 mg) was added. The reaction mixture was stirred for 30 min and kept in the dark overnight. Silica particles with porphyrin heterodimers were obtained after washing with Milli-Q water.

Transmission Electron Microscopy (TEM). TEM samples were prepared by dropping 10 μl aliquots of colloidal solution (ethanol/H_2O 1:1) onto a carbon-coated grid. After about 1 min, the remaining solution was blotted off with a filter paper. A Philips M12 transmission electron microscope operated at 100 kV was used to obtain the images of Figure 1.

UV/vis Spectroscopy of Silica Colloids. UV/vis absorption spectra of membrane coated silica colloids were acquired using a Perkin-Elmer Lambda 16 spectrometer.

Triplet absorption changes were measured with a conventional apparatus and signal averaging using 6-μs flashes. The oxygen was removed by bubbling with N_2. The triplet decay time did not change when the bubbling time was changed from 5 to 10 min.

Fluorescence Quenching Experiments. Fluorescence measurements and quenching experiments were performed on a Perkin-Elmer spectrometer (LS50B). Silica colloid coated with perforated membranes (3 mg) was dispersed in 3 mL of water and placed in a quartz cuvette. A 30 μl aliquot of the aqueous solutions of the quenchers such as a "fitting" porphyrin **7** (10^{-4} M), "too large" porphyrin **8** (10^{-4} M), 9,10-anthraquinone-2,6-diamine **10** (0.1 M), or 9,10-anthraquinone-2,6-disulfonic acid sodium salt **11** (0.1 M) was added. The fluorescence of bound bottom porphyrin on the particle surface was continuously checked. The same quenching procedure was used for amino functionalized particles and silica particles with preadsorbed porphyrin heterodimers.

Fluorescence decay measurements were carried out using the method of time-resolved single photon counting with equipment containing an SPC300 (Becker & Hickl) with a multichannel plate (Hamamatsu) and a Czerny−Turner monochromator (Oriel) on the detection pathway. For an additional exclusion of scattered light, a long-pass edge filter (530 nm) was used. As a light source, a TiSa-Laser (Mira 900, Coherent, duration 200 fs at 420 nm) was used. The sample was illuminated from below to optimize the coupling of the emitted light to the monochromator. The dimensions of the observed volume were reduced by long-distance focusing of the laser pulse into the sample and use of a 2-mm aperture directly in front of the sample. A response function of the setup shorter than 50 ps could thus be reached. The minimum time scale was also shortened by using deconvolution procedures to determine decay time values.

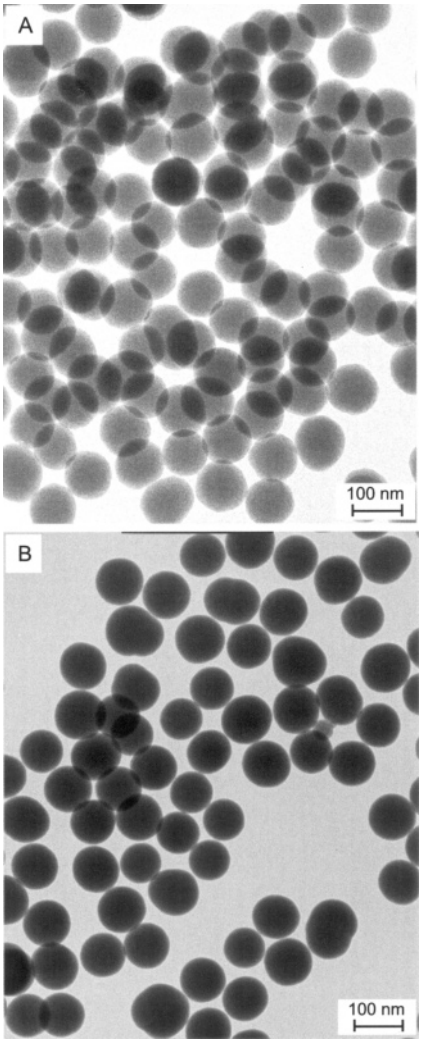

Figure 1. Transmission electron micrographs (TEMs) of synthetic silica particles (A) coated with $OSi-(CH_2)_3\ NH_2$ and (B) after two additional self-assembly steps with porphyrin **6c** first, followed by OEG-bolaamphiphile **5b**.

3. Results

We first tried to replace gold nanoparticles[5] with strong plasmon absorptions by presumably stable CabOSil colloids in water. This material is produced commercially by hydrolysis of silicon tetrachloride in a hydrogen flame at 1200 °C, does not contain pores, and can easily be functionalized with phosphonates and zirconium(IV) salts.[9] We examined the particles by transmission electron microscopy (TEM) and observed ill-defined networks of 20-nm spheres with a rough surface. The most disturbing property, which made these particles useless for our purpose, was the formation of large protrusions after treatment with silylated amphiphiles in organic solvents, in particular chloroform. The Si−O−Si networks seemed to swell extensively in chloroform and did not allow the formation of a stabilizing, closed monolayer of diamido lipids.[3]

We turned to the silicate particles developed by van Blaaderen, which are produced by hydrolysis of tetraethoxysilane (TEOS) with aqueous ammonia in ethanol and are stabilized by subsequent treatment with 3-aminopropyltriethoxysilicate.[10] We obtained spherical particles with a diameter between 20 and 150 nm depending on the concentration and hydrolysis time. The smaller particles showed, however, a rough surface in TEMs which was not appropriate for the self-assembly of rigid membranes and defined nanometer gaps.[11,12]The smallest uniform particles with a perfectly smooth surface had a uniform diameter of 100 ± 10 nm (Figure 1A). We optimized the conditions to produce them reproducibly in 1−10-g quantities and purified them by repeated precipitation at pH 2 and centrifugation, followed by redissolution at pH 11. These particles were stable and could be stored indefinitely as a moist powder. When resuspended in distilled water at pH 7−8, TEM always showed perfectly smooth particles even after the self-assembly of porphyrins and/or the amphiphilic monolayers (Figure 1B) described below.

The applied bolaamphiphiles **5a,b** with activated carboxyl and oligoethylene (OEG) end groups as well as an activated double bond for Michael addition to the eventual membrane gaps were synthesized by standard substitution, olefination, and condensation procedures. The applied porphyrins **6**−**9** have been described in the literature;[3,4] quinones **10** and **11** are commercially available (Scheme 1).

The two-step self-assembly to form rigid monolayered walls around a 2-nm gap with a porphyrin at the bottom was carried out as follows. The amine-coated silica particles were first dispersed in ethanol by mild sonication and centrifuged and redispersed 4 times. The same procedure was repeated with dichloromethane suspensions. The particles were finally suspended in dichloromethane containing triethylamine and mixed with 1 mg of the *meso*-(tetra-*m*-benzoyl chloride)porphyrin **6a** or the mixed tetraanhydride **6b** in 60 mL of dichloromethane. The particles, which are sketched in Figure 2a, remained soluble in dichloromethane as well as in water. If the corresponding octacarboxy porphyrin (OCP) with four *meta*-carboxy substituents on both sides of the porphyrin plane (not shown) was applied instead, the silicate particles aggregated strongly at all pH values between 2 and 12. It was thus not possible to bind this charged porphyrin onto the surface of the aminated silica particles. Negatively charged gold particles had not produced any problems.[5] After centrifugation and redispersion in dichloromethane, bolaamphiphile **5a** or **5b** was added and the solution was stirred overnight. The particles were now covered with an OEG surface and were still soluble in water. Addition of methylamine and subsequent centrifugation produced particles with a stiff coating of **5a,b** containing gaps around porphyrin **6c** at the bottom and a ring of methylammonium groups below the OEG headgroups (Figure 2b). The distance between the ammonium ring and the surface of the bottom porphyrin was measured in ChemDraw models as 10 Å in the case of the **5b** coating and 5 Å in the case of the **5a** coating. It was assumed that both the spacer of porphyrin (*m*-benzoic amide) and the OEG-diamide chain occurred as *all-anti* conformers. This seemed to be justified by our experience with fluorescence experiments using quencher molecules, which are smaller, exactly fitting or being too large to enter the 2-nm gap. The results (see for example Figure 6) clearly indicate that no measurable domain formation of the bottom porphyrin had taken place and that the walls of the gaps are neither fluid nor contain any irregular bents.

The Soret band of the silicate-bound porphyrintetraamide **6c** appears at 413 nm (half-width, 17 nm) which is similar to that of the tetraethylester **6** in ethanol (418 and 15 nm). The intensity

Scheme 1

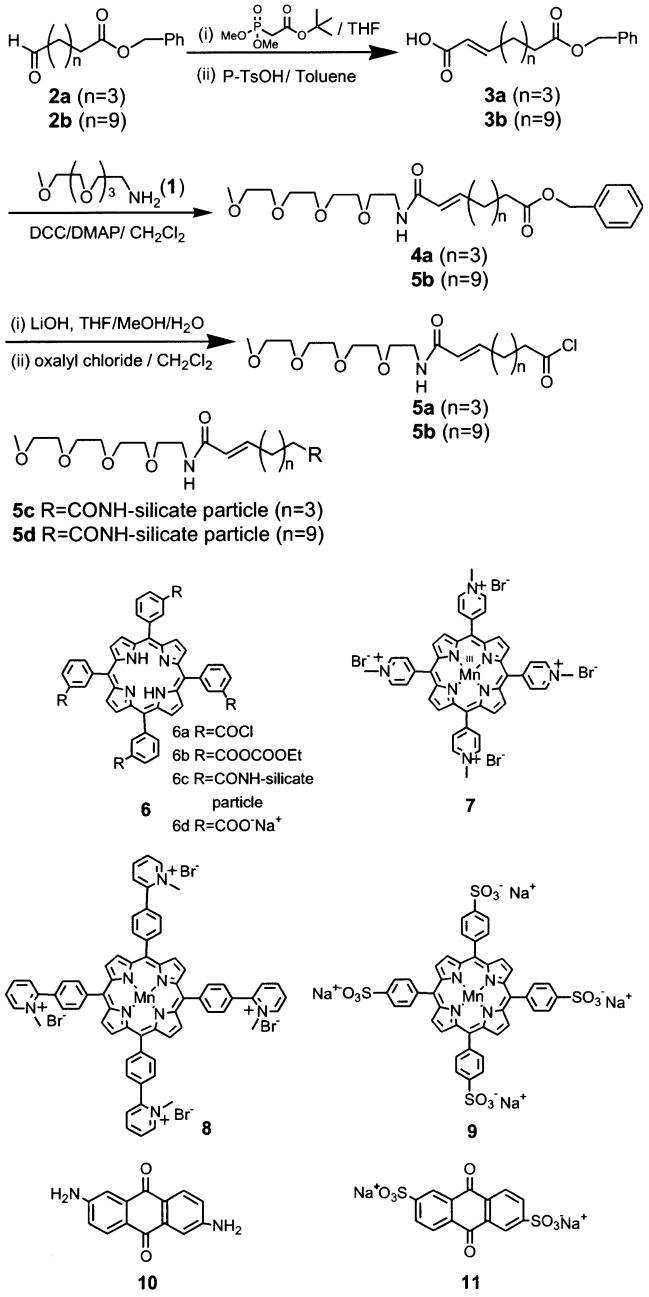

and line-width of the Soret band changed drastically upon aggregation of the aminated silica nanoparticles. At pH 11, the particles appear monomeric in TEMs, and the Soret band has a line-width close to that of monomeric TPP derivatives in solution, namely 17 nm. Upon acidification and formation of large numbers of cationic ammonium groups, we expected even better water solubility, but this was surprisingly not the case. At pH 7, the particles began to aggregate as indicated by TEM pictures as well as line-broadening in porphyrin spectra; the Soret band's half-width broadened from 17 to 34 nm. This could have been traced back to $NH_2 \rightarrow NH_3^+$ hydrogen bonding. At pH 3, however, where only well-hydrated NH_3^+ should be present, the particles even precipitated. Addition of sodium hydroxide lead to a quantitative reversal of the aggregation, and the half-width of the Soret band goes back to 17 nm at pH 11-(Figure 3). The Q-band near 550 nm was more sensitive to changes in the environment than the Soret band. **6c** absorbs at 549 nm in ethanol, at 557 in water, and at 552 nm in the water-filled nanowell.

The triplet state difference spectra of **6c** in the water-filled nanowell and of TPP in benzene are also quite similar. The maximum at 784 nm (Figure 4a, insert) is characteristic for the triplet absorption of tetraphenylporphyrin.[13] The halftime of the relaxation depends on the age of the preparation. In fresh preparations, the decay of the absorption change measured under nitrogen was nearly exponential with a half time of 85 μs (overall concentration of porphyrins $C_p = 2.1 \times 10^{-6}$ M, 1% excitation). This value was obtained with fresh probes made with the acid chloride **6a**, which is known to contain porphyrin domains, as well as with the mixed anhydride **6b**, which produces exclusively 2-nm-wide wells. Aged preparations ($t =$ 2 and 22 days) showed a nonexponential decay, which was not analyzed in detail. The first halftimes were 230 μs ($C_p = 2.6 \times 10^{-6}$ M, 2.5% excitation) and 860 μs ($C_p = 2.3 \times 10^{-6}$ M, 5% excitation). A comparison with literature triplet decay traces[14] in solution suggests that porphyrins with a stiff macrocycle, rigidified for example by central zinc ions or electron-withdrawing functional groups, exhibit a slow relaxation, whereas this process is accelerated in less rigid rings with better matching of the vibrational levels of the ground and triplet states. We measured 80 μs for the monomeric carboxylate **6d** in water, and literature reports give values between 110 and 800 μs for *o*,*m*,*p*-isomers of *meso*-tetra(methylpyridinium)porphyrins in water. If we compare these data with those of our porphyrin systems, then the fast relaxation of the monomers may be explained by the vibrational capabilities of the macrocycle, induced by free *m*-carboxyl groups of the phenyl rings, the triplet-stabilizing effect on the aged surface by immobilization through additional amide bonds.

o-Naphthoquinone sulfonate was then applied as a quencher of the triplet state. It accelerated the decay of the triplet absorption from 860 μs to 62 μs in the aged preparation and from 230 μs to 58 μs in an intermediate age. This corresponds to quenching constants of $k_q^T = (4-6) \times 10^7$ M^{-1} s^{-1} ($C_q = 3.1 \times 10^{-4}$ M). The amplitude of the absorption decreased, indicating quenching of the singlet state also. The Stern−Volmer constant was $(5-6) \times 10^3$ M^{-1}. Stern−Volmer traces for anthraquinone disulfonate **11**, naphthoquinone sulfonate NQS^-, and methyl viologen MV^{2+} indicate that the redox potential of the excited singlet state of **6c** is negative enough to reduce **11** and even methyl viologen. Oxidative quenching is exergonic for all three ($\Delta G_o = -0.29$, -0.72, and -0.23 eV). The triplet state reduction power is lower by 0.47 eV and allows the reduction of NQS^- but not of **11** or MV^{2+} (Figure 4b).

The absorption and fluorescence spectra of the adsorbed porphyrin hardly change after the second self-assembly step of bolaamphiphiles around the porphyrin. Only a negligibly small blue shift was observed. The porphyrin **6c** at the bottom of a rigid membrane gap is difficult to reach by large solutes in the bulk water phase. Fluorescence quenching with water-soluble manganese porphyrins **7** and **9** occurs immediately ($\ll$1 s) if the porphyrin is bound to the aminated silicate without a surrounding wall (see model in Figure 2a). If it is fenced in (Figure 2b), maximal quenching is only reached after ~50 min. It takes a long time until the manganese porphyrin molecules

(14) (a) Kalyanasundaram, K.; Neumann-Spallart, M. *J. Phys. Chem.* **1982**, *86*, 5163. (b) Kalyanasundaram, K. *Inorgan. Chem.* **1984**, *23*, 2453.

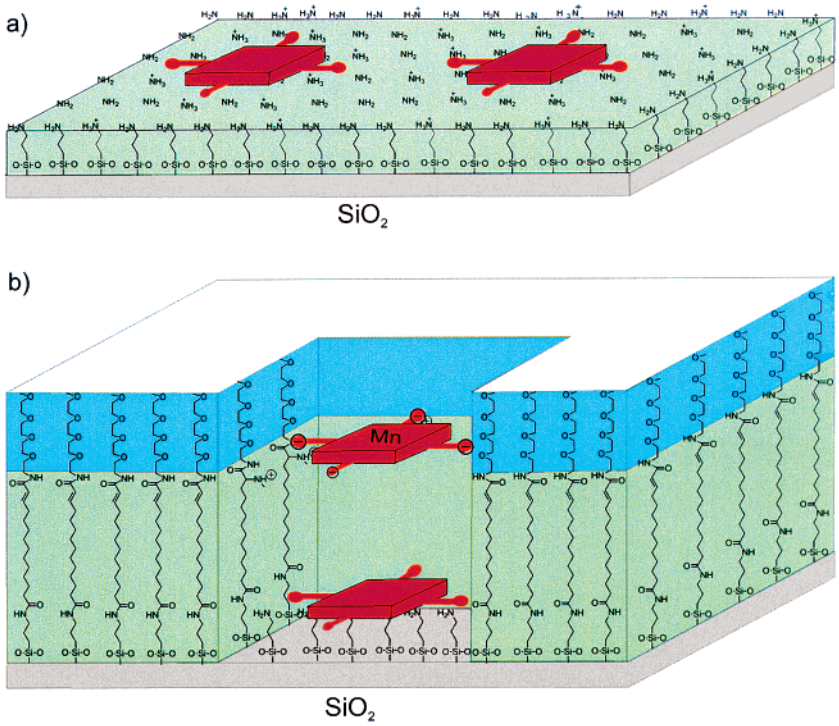

Figure 2. Model of the target silica particles (a) coated with propylamine-triethoxysilicate and porphyrin **5c**, (b) after the second self-assembly of OEG-bola **5b**. Methylamine was also covalently attached to the double bonds facing the gap, and a second porphyrin was fixated above the methylammonium ring.

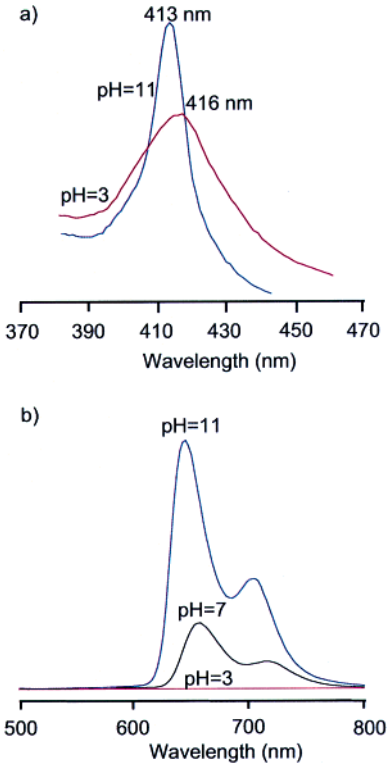

Figure 3. (a) Absorption and (b) fluorescence spectra of the silicate particles shown in Figure 2a at different pH values. More NH_3^+ groups lead to more hydrogen bonds and to aggregation, to a broadening of absorption peaks and to a loss of fluorescence. The aggregation of the particles was fully reserved at pH 11 after addition of NaOH.

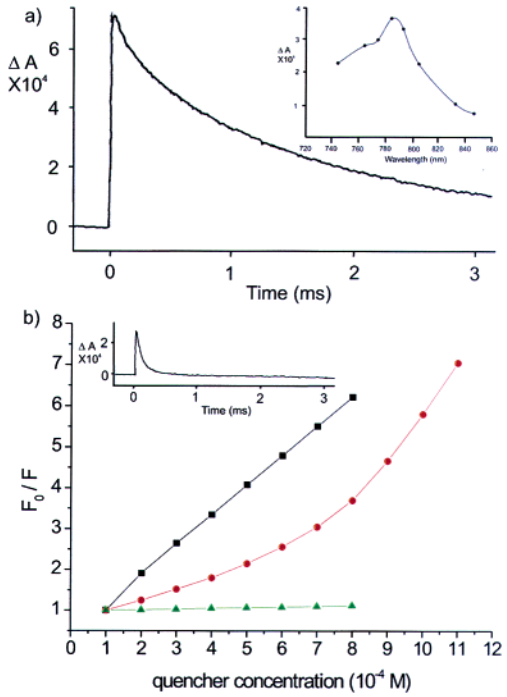

Figure 4. (a) Triplet spectrum (insert) and decay of porphyrin **6c** on silica. (b) Decay of the triplet state of **6c** in the presence of naphthoquinone sulfonate (insert) and Stern−Volmer plots of titrations with anthraquinone-disulfonate **11** (■), naphthoquinone-4-sulfonate (●), and dimethyl viologen (◆).

find their way to the bottom of the 2-nm well (Figure 5); the curve is not exponential.

Porphyrins, whose diameter is larger than the well, for example, **8**, should not reach the bottom at all. It proved, however, to be difficult to demonstrate this filter effect with the silicate particles. It did not work at all when the porphyrin tetraacyl chloride **6a** was used in the first self-assembly step. This activated porphyrin presumably formed domains on the silicate surface rather than spots of monomeric porphyrins, because it readily formed anhydride dimers upon partial hydrolysis of the acid chlorides, which could not be totally

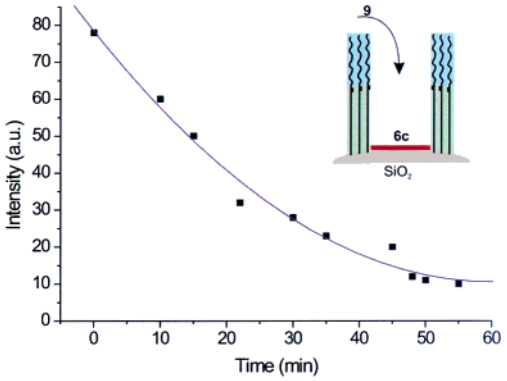

Figure 5. Time-dependent fluorescence quenching after addition of Mn-(III) TPPS **9** (10^{-6} M) to porphyrin **6c** entrapped on the silica surface by **5b**. It took ~20 min to reach 50% of the maximum quenching.

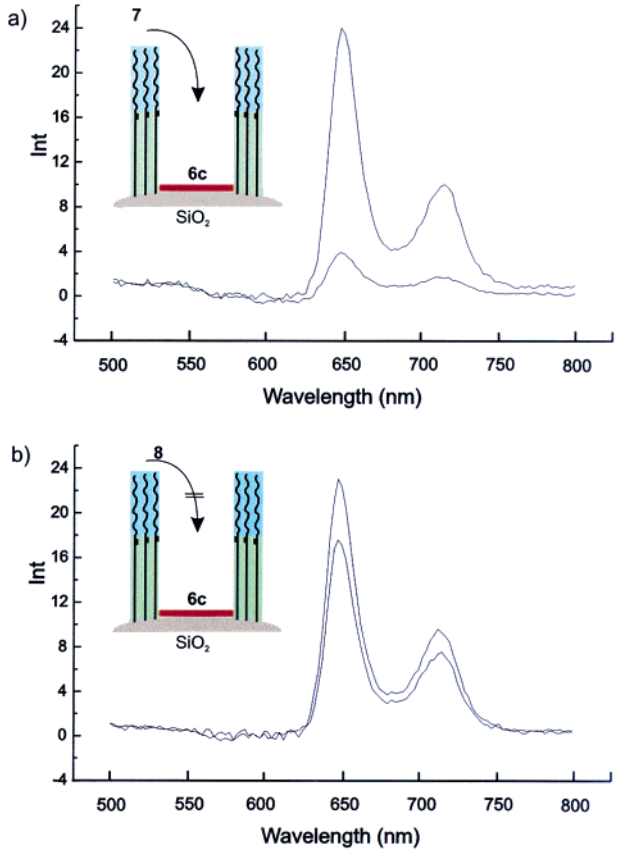

Figure 6. Fluorescence quenching of the porphyrin **6c** surrounded by rigid walls with (a) the Mn(III) porphyrin **7** fitting into the gap and (b) the porphyrin **8**, which is too large. The rest fluorescence in part a indicates dynamic quenching by **7**; the partial quenching in part b may be caused by domain formation of the bottom porphyrin.

avoided. The more stable mixed anhydrides **6b** made with ethyl chloroformate were much more reliable. Gaps based on the acid chloride porphyrins hardly differentiated between manganese porphyrins **7** and **8** with diameters of 2.0 and 3.6 nm, whereas gaps produced with the corresponding anhydrides filtered the large porphyrin off with an efficiency of 80% (Figure 6). The rest (20%) are probably caused by some dimeric or more highly aggregated bottom porphyrin domains. It also turned out that charge interaction between positively charged quencher molecules and a negatively charged bottom porphyrin was not necessary for efficient quenching within the nanometer gaps. The bottom porphyrin **6c** was electroneutral and combined

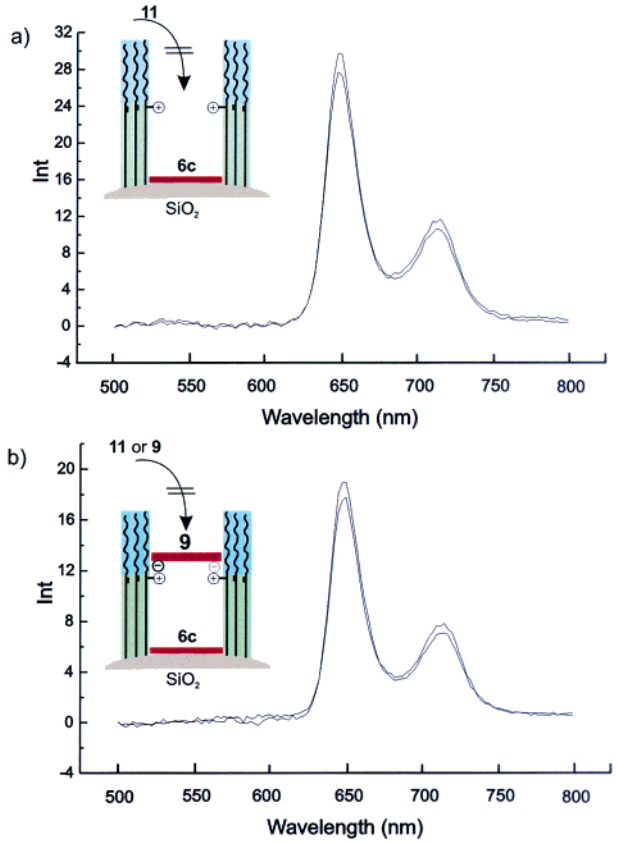

Figure 7. Figure 7. Fluorescence quenching of porphyrin **6c** by addition of (a) 10^{-6} M quinone disulfonate **11** (compare with Figure 6) and (b) Mn-(III) TPPS **9** (compare with Figure 7) after Michael addition of methylamine to the double bonds facing the gap. (b) Addition of a large excess of manganese porphyrin **9** or quinone **11** to the porphyrin-covered sample does not lead to fluorescence quenching of the bottom porphyrin. Both porphyrin **9** and quinone **11** covers close the gap reversibly. Addition of sodium hydroxide to the bulk water neutralizes the positive charges and opens the gap again.

readily with porphyrin cation **7** as well as with anion **9**. Quenching occurred to an extent of about 90%.

The disulfonated anthraquinone **11** passed the OEG headgroup and entered the pore rapidly. There was no measurable difference between porphyrin **6c** lying freely accessible on the amine surface and the fenced-in porphyrin. This changed drastically with the diaminoanthraquinone **10**. It had a strong quenching effect on porphyrin **6c**, which was in direct contact with the bulk water (not shown) and did not reach **6c** at the bottom of the gap at all. This indicates that the amino groups formed a molecular complex with the OEG headgroups, which did not allow any transport of quencher molecules into the pore. The aminoanthraquinone **10** is thus bound in unknown orientations at a distance of 12 Å from the bottom porphyrin and could act as an electron acceptor as well as a cover of the gap. Addition of a large excess of sulfonated naphtho- or anthraquinones had a quenching effect of much less than 10%, when added after this cover molecule.

We have shown earlier that tyrosine and other rigid edge amphiphiles are fixated to the walls of water-filled hydrophobic nanometer gaps and block the diffusion of porphyrins into the nanowells.[3,4,17] This property is also realized on silica. The

(15) Weisbecker, C. S.; Merritt, M. V.; Whitesides, G. M. *Langmuir* **1996**, *12*, 3763.

Table 1. Fluorescence Decay Times

sample	τ_1 [ns]	τ_2 [ns]	τ_3 [ns]	relative amplitudes
porphyrin **6d** (aq soln)	10.1 ± 0.5			
6c (on silica with or without Michael addition on monolayers of **5a** or **5b**)	9.3 ± 0.8	1.6 ± 0.3		1:/between 0.2 and 1
6c with Mn(III) TPPS at 5 Å	8.6 ± 0.8	1.4 ± 0.3	0.16 ± 0.10	1/0.2−1/2,4
6c with Mn(III) TPPS at 10 Å	9.5 ± 0.8	1.6 ± 0.3		1:1 or smaller

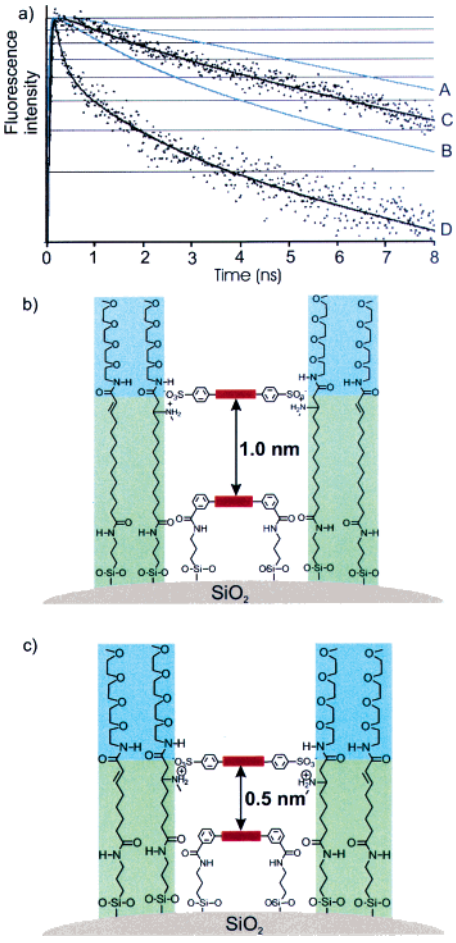

Figure 8. Figure 8. (a) Trace A and C are blanks. Trace A shows the decay of **6c** on naked, aminated silicate particles (see model in Figure 2a); trace C is the whole system with **6c** and bola **5c** (see model in Figure 2b). Traces B and D were obtained after fixation of Mn(III) TPPS at a distance of 10 and 5 Å (see models in parts b and c). Only trace D indicates an effect of Mn(III) TPPS, namely 60% decay after 0.16 ns. (b) Model of the 1.0-nm heterodimer **6c**−**9** (trace B). (c) Model of the 0.5-nm heterodimer **6c**−**9** (trace D).

particles with a coating made of porphyrin **6c** and bola **5d** were stirred overnight in a 0.05 M solution of tyrosine, centrifuged, redispersed, and centrifuged twice in distilled water, and their fluorescence was measured. It was within a possible error of ±20%, the same as that before addition of tyrosine. Addition of a large excess of quinones **11** or Mn(III) TPPS **9** did not diminish the fluorescence at all; the pore was irreversibly clogged under these conditions.

The aminated silica particles covered with porphyrin **6c** surrounded by bolaamphiphile **5d** walls were then functionalized at the double bond by Michael addition of methylamine. A ring of methylammonium groups was formed directly below the OEG headgroups. The disulfonated anthraquinone **11** and the manganese(III) tetraphenylsulfonate porphyrin **9**, which was added to the bulk water solution, were now also bound at the rim of the gap. Less than 10% quenching of the fluorescence was observed (Figure 7); addition of a large excess of NQS^- or quinone **11** had no effect. The absorption spectrum of centrifuged and redispersed particles showed the quinone or manganese porphyrin absorption bands next to the Soret band of the bottom porphyrin **6c** (not shown). Three long-distance redox pairs of **6c** with two anthraquinones of different oxidation potentials and one metalloporphyrin were thus established.

We then studied the behavior of the excited singlet state of the bottom porphyrin **6c** in the absence or presence of Mn(III) TPPS **9** at a distance of 10 Å or 5 Å. The excited singlet state of **6c** was therefore produced with 200-fs pulses at 420 nm, and its decay time was measured. The blank experiments without the distant manganese porphyrin showed two typical times of decay of ∼8 ns and 1.6 ns, which we always found on the silicate particles. Fixation of Mn(III) TPPS **9** at a distance of 10 Å also had no effect. The three traces, before and after addition of methylamine and **9**, were close to identical; slight decreases in intensity were within the experimental error between different blanks. In the case of the 5 Å distance, however, the decay time became faster by about 15% and, more significant, a new decay mechanism was established with a decay time of about 0.2 ns (Figure 8a, Table 1). This is in agreement with the slowest times measured for electron transfer in photosynthesis and in covalent model systems. The finding that the same redox pair showed no interaction at all, when kept at an intermolecular distance of 10 Å, indicates, however, another quenching mechanism, probably energy transfer. The same experiments with the triplet excited states showed no such short decay time.

4. Discussion

Protection of the silicate surface by the thin propylamine coating as introduced by van Blaaderen[10] solved the major problems, which were encountered with commercial $CabOSil^-$ and citrate gold particles: (i) no detectable roughness or irreversible aggregation occurred, (ii) organic solvents did not cause any swelling or formation of jelly like protrusions, (iii) self-assembly processes on the amino surface gave closed rigid monolayers with form-stable gaps (ill-defined, larger gaps occurred only to an acceptable extent of about 10%), (iv) no disturbing photochemistry of the carrier competed with that of the adsorbed dyes, and (v) the electroneutral porphyrin spots on the amine surface did not intervene with reversible precipitation−dissolution cycles upon pH changes (Figure 2).

There arose, however, also two problems with the described silica particles. Because of the large diameter of the particles,

(16) Träger, O.; Sowade, S.; Böttcher, Ch.; Fuhrhop, J.-H. *J. Am.Chem. Soc.* **1997**, *119*, 9120.
(17) Li, G.; Doblhofer, K.; Fuhrhop, J.-H. *Angew. Chem.* **2002**, *114*, 2855; *Angew. Chem., Int. Ed.* **2002**, *41*, 2730.

which could not be avoided, less than 1 mg of porphyrin is bound to 100 mg of SiO_2; the attainable porphyrin concentration was less than 10^{-5} M. Second, one cannot apply dyes with negative rest charges, which would be helpful in the establishment of strongly coupled molecular systems, for example, the packing of three or more components into the well. The problem of low concentration was overcome be applying only emission spectroscopy as an analytical tool, and the lack of charged porphyrins had fortunately no serious consequences for fluorescence quenching experiments. It turned out that the van der Waals interactions between dye molecules are sufficient for strong quenching effects within the hydrophobic nanowells in aqueous media. Both the tetracationic porphyrin and the dianionic anthraquinone found their way to the electroneutral porphyrin on the amine surface as well as at the bottom of the gaps.

The aminopropyl-coated silica particles flocculated only slowly (>3 h) in water at pH 11 and not at all when 50% ethanol was added to this solution. Ionization of the amino groups had, surprisingly, no stabilizing effect. On the contrary, at pH 3, immediate and complete coagulation took place. Similar observations have been made with propionate-coated gold particles. These particles coagulated rapidly independent of ionization of the coating. Only hydroxylation of naked gold colloids had a strong stabilizing effect above pH 11.[15] We assume that the aminated silica particles also add hydroxyl ions, which deprotonate some remaining Si−OH groups forming silicate anions next to the NH_2 groups. Repulsive interactions between these hidden negative charges then prevent coagulation. The extra stabilization by ethanol is probably caused by solvation of the propyl groups. At low pH, the silicate layer is probably protonated and loses its repulsive character, whereas the ammonium polyelectrolytes stick together via ion pairs and hydrogen bonding. This corresponds to the cationic analogue of acid soaps.[16]

After amidation of the amino groups with porphyrin **6b** and bolaamphiphiles **5a,b**, the solubility of the particles became pH independent. Interactions of the porphyrin on the bottom of the nanowell with water-soluble, redox-active molecules were now studied at pH 7−8 by fluorescence measurements.

The aminoanthraquinone **10** was stopped by the OEG headgroups at the entrance of the gaps, whereas the corresponding sulfonate **11** passed freely and caused 90% fluorescence quenching, when used in excess. **11** was also stopped, when a methylammonium ring was introduced at the entrance of the hydrophobic part of the gap. The distance between **10** at the top and **6c** at the bottom of the nanowell should be close to 5 Å in the case of **5c** walls and 10 Å in the case of **5d**. The orientation of the quinone is, however, not known. Since its size is not sufficiently large to interact with ammonium groups on opposite sites of the circle, it may stick to the hydrophilic or hydrophobic parts of the wall like a painting or float in water like a sea flower. Transient emission spectroscopy experiments with fixated **10** and **11** showed, however, only dynamic quenching; no defined new decay mechanism was observable. Stern−Volmer plots of the systems with and without trapping effects of the gap's entrance looked similarly. We conclude that neither the ammonium sulfonate charge interaction nor the OEG−ammonium bonds are stable enough in water to withstand slow substitution by anthraquinone sulfonate or amine molecules, which are present in the bulk solution. Such substitution reactions may push the quinones into the gap. This process was, however, completely inhibited if the gap was filled with 0.1 M tyrosine solution before. Binding of the electron acceptors to the headgroups combined with a blockade by tyrosine or cellobiose[17] may thus produce stable systems. We did not examine this possibility, because the anthraquinones did not promise well-defined acceptor sites with respect to position and distance.

We limited ourselves to further experiments with the much more stable heterodimer with Mn(III) TPPS **9**. It is of interest for two reasons: it allows the study of one-dimensional diffusion, and it can be cemented in its position by a ring of methylammonium groups, because it fits exactly into the 2-nm gaps.

The diffusion of **9** into the gap with a depth of about 1.0 nm takes about 20 min and can thus be easily followed by standard fluorescence spectroscopy (Figure 5). The gap-fitting porphyrin quenched the bottom porphyrin's fluorescence to the same extent as 90% of the porphyrin on the amine surface. This indicates a "limited reversibility" of the complex formation at the bottom of the gaps. The heterodimer can dissociate, but the second component does not leave the pore. The system is interesting, because it allows us to study the kinetics of one-dimensional diffusion in aqueous solution systematically. It is known that the diffusion coefficient for porphyrin disks in a small, liquid-filled pore is smaller than the value for bulk solution, when the molecule and the pore are of comparable dimension. Viscous retardation and unfavorable partition are possible mechanisms.[18] The pores, which were investigated so far, had, however, a molecule/pore size ratio λ of about 0.2. Diffusion was still very fast. In the Mn(III) TPPS **9** case, λ approaches 1, and the diffusion constant should approach zero. A diffusion pathway of about 1 nm in 20 min is close to that prediction. The only free room for solvent passage is around the phenyl substituents, which are oriented at angles between 60 and 90° with respect to the porphyrin plane. To the best of our knowledge, no other nanowell or pore has slowed the one-dimensional diffusion to this extent. The rigid and tailored 2-nm wells on soluble particles with a sensitive fluorescence indicator at the bottom provide a unique possibility to study one-dimensional sliding movements of molecules along walls, whose properties can be modified. Smaller quenchers will allow comparisons with standard one-dimensional diffusion experiments. Fitting pore-entrapped molecules are also of interest, because they appear as isolated monomers. Radicals may become quite stable here.

We also consider experiments concerning two-dimensional diffusion processes. The approaching quencher may or may not be adsorbed by the silicate particle and may reach the gaps' entrance directly from the bulk solution by three-dimensional diffusion or after migration on the particles' surface by two-dimensional diffusion. To analyze the results, one needs to know the number of gaps per silica particle, and this cannot be determined directly. It is, however, easy to vary the number of gaps by a change of self-assembly times and obtain occupancy ratios from the intensity of the Soret band in different preparations. Furthermore, the amino silica particles are soluble in water and many solvents, and the chemistry of the amino groups is

(18) Kathawalla, I. A.; Anderson, J. L.; Lindsey, J. S. *Macromolecules* **1989**, *22*, 1215.

versatile enough to produce all kinds of surfaces. So far, we have only been using oligoethylene glycol, because it is soluble in water as well as in several solvents. Charged, chiral hydrogen bonding and complex forming headgroups on the silica surfaces will produce particles, which bind, reject, or allow two-dimensional diffusion of quencher molecules. By changing both, the number of nanowells and the properties of the surfaces, we find it thus becomes possible to study two-dimensional diffusion in a general manner. So far, the systems for two-dimensional diffusion have provided a limited versatility, for example, vesicle membranes,[19] described only reaction rates,[20,21] or were theoretical models only (butterfly antennae,[22] fractal aggregates[23]).

Coming back to the fixated Mn(III) TPPS **9** electron acceptor, we first review shortly what is known about long-distance electron transfer (ET) reactions between porphyrin donor−acceptor (DA) or donor−bridge−acceptor (DBA) redox pairs. They have been studied in photosynthetic membrane proteins containing chlorophyll, pheophorbide, and quinones as well as in covalent models.[24−28] The theory of ET reactions was summarized by Wasielewski.[29] It implies a steep distance dependence in absence of electronically coupled bridges with a fitting energy gap. In the words of an old dictum of Mauzerall:[30] "The probability of electron tunneling is a powerful function of the distance, and the requirement of trapping creates a sharp maximum. Too far, and the probability of electron transfer is too low during an excited state lifetime. Too close, and the back transfer to the ground state becomes too fast". A distance of 20 Å was taken as an upper limit for fast transfer in lipid membranes, and ∼10 Å should be ideal for "gated" electron transfer in a one-way direction only. This was the base of our building plan.

In the nanowells, an amorphous rigid water volume separates the redox pair. Modification of the site of the double bond site allows variations of the distance between electron donor and acceptor in steps of 2.5 Å. This limit is caused by the requirement that the number of CH_2 groups between the two secondary amide groups must be even. Therefore, two CH_2 groups must be added or subtracted in the separating chain. The concentration of both porphyrins **6c** and **9** was about 10^{-6} M and not sufficient for transient absorption spectroscopy with our equipment. We used therefore transient emission spectroscopy. Surprisingly, no effect of Mn(III) TPPS **9** was observed at a 1.0-nm distance. Essentially the same decay times of 9.5 and 1.6 ns were observed with and without Mn(III) TPPS. A similar biphasic behavior has been reported for porphyrin monolayers, which were separated by lipid monolayers from the gold surface of nanoparticles.[31] A new, faster, and very efficient decay mechanism with a decay time of 0.16 ns only appeared, when the manganese(III) porphyrin was attached at a distance of 0.5 nm. A time of 160 ps is in agreement with rates of electron transfers in the slowest model systems.[25,29] This slowness could correspond to the unexpected finding, that the potential barrier for electron tunneling[32,33] in the water-filled gaps is so high that a distance of 1.0 nm cannot be overcome. A more likely explanation is nonefficient energy transfer, which may be expected in nonorganized, aqueous systems.[34]

5. Conclusion

The aminated silica particles introduced by van Blaaderen proved to be an exceptionally stable and versatile substrate for the establishment of rigid, closed membranes containing form-stable nanometer gaps and photoactive heterodimers in aqueous media and organic solvents. Their photochemical and electronic inertness limits their usefulness to that of a carrier system with a smooth and reactive surface, but in this respect, they are unsurpassed by any other colloidal particle. 1D and 2D diffusion and charge separation experiments with noncovalent long-distance heterodimers become routine experiments using these particles and a fluorescence spectrometer. For experiments concerning charge separation between heterodimers, the bottom porphyrin will be converted to zinc- or tin(IV) complexes in order to function as donor or acceptor, and charged acceptor and donor molecules of the same size must be synthesized. Work along these lines is in progress.

Acknowledgment. Financial support by the Deutsche Forschungsgemeinschaft (SFB 348 "Mesoscopic Systems"), the European TMR research network "Carbohydrate Recognition", the Fonds der Deutschen Chemischen Industrie, and the FNK of the Free University is gratefully acknowledged. We also thank Dr. Jörg Zimmermann, Berkeley for helpful discussions.

JA035558W

(19) (a) Naqvi, K. R.; Martins, J.; Melo, E. *J. Phys. Chem. B* **2000**, *104*, 12035. (b) Martins, J.; Naqvi, K. R.; Melo, E. *J. Phys. Chem. B* **2000**, *104*, 4986.
(20) Somorjai, G. A. *Chemistry in Two Dimensions: Surfaces*; Cornell University: Ithaca, NY, 1981.
(21) Engel, T.; Ertl, G. *Adv. Catal.* **1979**, *28*, 1.
(22) Adam, G.; Delbrück, M. Reduction of Dimensionality in Biological Diffusion Processes. In *Structural Chemistry and Molecular Biology*; Rich, A., Davidson, N., Eds.; W. H. Freeman and Company: San Francisco and London, 1968.
(23) Yang, C.-L.; Chen, Z.-Y.; El-Sayed, M. A. *J. Phys. Chem.* **1987**, *91*, 3002.
(24) Deisenhofer, J.; Epp, O.; Miki, K.; Huber, R.; Michel, H. *J. Mol. Biol.* **1984**, *180*, 385.
(25) Kurreck, H.; Huber, M. *Angew. Chem., Int. Ed. Engl.* **1995**, *34*, 849.
(26) Gust, D.; Moore, T. A.; Moore, A. L. *Acc. Chem. Res.* **2001**, *34*, 40.
(27) Sessler, J. L.; Johnson, M. R.; Lin, T.-Y. *Tetrahedron* **1989**, *45*, 4767.
(28) Osuka, A.; Marumo, S.; Mataga, N.; Taniguchi, S.; Okada, T.; Yamzaki, I.; Nishimura, Y.; Ohno, T.; Nozaki, K. *J. Am. Chem. Soc.* **1996**, *118*, 155.
(29) (a) Miller, S. E.; Lukas, A. S.; Marsh, E.; Bushard, P.; Wasielewski, M. R. *J. Am. Chem. Soc.* **2000**, *122*, 7802. (b) Wasielewski, M. R. *Chem. Rev.* **1992**, *92*, 435.
(30) (a) Mauzerall, D.; Hong, F. T. In *Porphyrins and Metalloporphyrins*; Smith, Ed.; Elsevier: Amsterdam, 1975. (b) Mauzerall, D. In *Photoinduced Electron Transfer, Part A*; Fox, M. A., Chanon, M., Eds.; 1988; p 228.
(31) Imahori, H.; Arimura, M.; Hanada, T.; Nishimura, Y.; Yamazaki, I.; Sakata, Y.; Fukuzumi, S. *J. Am. Chem. Soc.* **2001**, *123*, 335.
(32) Moser, C. C.; Page, C. C.; Chen, X.; Dutton, P. L. *J. Biol. Inorg. Chem.* **1997**, *2*, 393.
(33) Page, C. C.; Moser, C. C.; Chen, X.; Dutton, P. L. *Nature* **1999**, *402*, 47.
(34) Van Patten, P. G.; Shreve, A. P.; Donohoe, R. J. *J. Phys. Chem. B* **2000**, *104*, 5986.